Fabrication of bulk amorphous $Fe_{67}Co_{9.5}Nd_3Dy_{0.5}B_{20}$ alloy by hot extrusion of ribbon and study of the magnetic properties

K. BISWAS*
Leibniz-Institut für Festkörper- und Werkstoffforschung Dresden, Helmholtzstr. 20, D-01069, Dresden, Germany

S. RAM
Materials Science Centre, Indian Institute of Technology, Kharagpur 721302, India

S. ROTH, L. SCHULTZ
Leibniz-Institut für Festkörper- und Werkstoffforschung Dresden, Helmholtzstr. 20, D-01069, Dresden, Germany

J. ECKERT
FG Physikalische Metallkunde, FB 11 Material- und Geowissenschaften, Technische Universität Darmstadt, Petersenstr. 23, D-64287, Darmstadt, Germany

Published online: 12 April 2006

We report on the preparation of bulk amorphous $Fe_{67}Co_{9.5}Nd_3Dy_{0.5}B_{20}$ by hot extrusion of melt-spun ribbons. X-ray diffraction studies were performed to check the structure of the as-spun ribbons and the consolidated bulk specimens. Differential scanning calorimetry (DSC) analysis of the amorphous ribbons revealed that crystallization proceeds in two stages. The first crystallization step leads to the formation of soft magnetic α-(FeCo) and $(FeCo)_3B$ and the second crystallization step corresponds to the formation of the hard magnetic $(NdDy)_2(FeCo)_{14}B$ phase. The hysteresis loop of the as-spun ribbon reveals soft magnetic properties which change to hard magnetic behavior with enhanced remanence after annealing at 973 K for 7 min. X-ray diffraction analysis proves the presence of both soft and hard magnetic phases in the annealed sample. The viscosity of the powder obtained from crushed ribbons was investigated by parallel plate rheometry, showing a distinct viscosity drop in the supercooled liquid region that allows for easy consolidation of the crushed ribbons. The hot extruded sample that was subsequently annealed at 973 K for 7 min exhibits good hard magnetic properties with coercivity $H_c = 218$ kA/m, saturation magnetization $J_s = 1.36$ T, maximum energy product $(BH)_{max} = 91.3$ kJ/m^3 and remanence $B_r = 1.18$ T (after demagnetization field correction), respectively.

1. Introduction

Over the last years, the excellent hard magnetic properties of Nd-Fe-B alloys containing mainly the $Nd_2Fe_{14}B$ compound as hard magnetic phase have been thoroughly studied [1–5]. In particular, exchange-coupled nanocomposite permanent magnets consisting of the hard magnetic $Nd_2Fe_{14}B$ and soft magnetic α-Fe or Fe_3B phases have attracted attention due to their superior magnetic properties [6–11]. Besides, Zhang *et al*. reported good hard magnetic properties for optimally annealed amorphous Fe-Co-Nd-Dy-B ribbons due to the exchange coupling between hard and soft magnetic phases [12, 13]. The hard magnetic properties are interpreted to result from the exchange coupling between $(NdDy)_2(FeCo)_{14}B$, α-(FeCo), $(FeCo)_3B$ and the remaining amorphous phases.

Besides attempts to directly cast bulk samples, where the hard magnetic properties were tuned in by appropriate heat treatment [13], Ishihara *et al*. [14] and Parida *et al*. [15] succeeded in producing consolidated bulk material from melt-spun amorphous $Fe_{67}Co_{9.5}Nd_3Dy_{0.5}B_{20}$

*Author to whom all correspondence should be addressed.
0022-2461
DOI: 10.1007/s10853-005-5619-z

ribbons by hot pressing techniques. The thermal stability of the supercooled liquid, the crystallization products, and the magnetic properties of this alloy were studied by Zhang *et al*. [12, 13]. However, there are no reports on the preparation of consolidated bulk samples from melt-spun amorphous $Fe_{67}Co_{9.5}Nd_3Dy_{0.5}B_{20}$ ribbons by hot extrusion. The densification degree upon extrusion is much higher than for hot pressing techniques [16]. Additionally, the tendency of forming pores for hot pressed samples leads to a possible nonhomogeneous consolidation, which can be avoided by hot extrusion [16] with a lower residual porosity.

A recent crystallization kinetics study [17] showed that the activation energy for this alloy is much higher than that of $Fe_{80}B_{20}$. The substitution of Fe by Co, Nd and Dy results in higher thermal stability and resistance to crystallization. This is beneficial for producing bulk amorphous samples by extrusion of pieces of melt-spun amorphous ribbons. This is of particular interest, since it was not possible to fabricate cylinders of more than 0.5 mm diameter by conventional copper mold casting because of the limited glass-forming ability (GFA) of this alloy [13]. Hence, the alternative way of preparing bulk amorphous samples by a combination of rapid quenching, ball milling and hot working processes seems to be a promising route for the preparation of bulk specimens without limitation of size or geometry [18]. Together with appropriate annealing to induce the formation of hard magnetic phases, this may yield bulk specimens with interesting magnetic properties. Accordingly, the present work is focused on the preparation of bulk amorphous samples by extrusion of amorphous ribbons and reports on the achievable magnetic properties of amorphous ribbons and extruded bulk samples.

2. Experimental

A master alloy of the desired composition of $Fe_{67}Co_{9.5}Nd_3Dy_{0.5}B_{20}$ was prepared by arc melting the mixture of the pure metals (Fe: 99.99% purity, Co: 99.99% purity, Dy: 99.99% purity, Nd: 99.99% purity) and FeB (18.6 wt.% B: 99.9% purity) in an argon atmosphere. From this master alloy amorphous ribbon with a thickness of about 55 μm was prepared by melt spinning in an Ar atmosphere using a wheel speed of 14.4 m/s. Some parts of the ribbon were cut into small pieces (2.5 cm long) for further ball milling.

A Retsch PM400 planetary ball mill was used to crush the ribbon which was cut beforehand into small pieces. These experiments were done with a powder-to-ball mass ratio of 1:10 at a speed of 300 rpm/min under reversible mode. The milling time was 15 min to guarantee that no significant structural changes occur during milling [14]. The vials were opened after appropriate periods of processing under an argon atmosphere. This powder was later used for the extrusion experiments.

The viscosity of the $Fe_{67}Co_{9.5}Nd_3Dy_{0.5}B_{20}$ powder in the supercooled liquid region was determined by parallel plate rheometry using a thermal mechanical analyzer (Perkin-Elmer TMA 7) according to Stefan's equation [19–20]. The measurements on the powder samples were conducted under argon atmosphere at a heating rate of 40 K/min using quartz penetration probes (3.7 mm diameter) as parallel plates and a static force of 2.6 N [21, 22].

The compaction of the powders was done by extrusion using a Weber hot press facility and a specially designed extrusion die inserted into the hot press. In the first step the crushed powders were cold compacted into green bodies under argon atmosphere, which were then encapsulated into copper cans (12 mm outer and 10 mm inner diameter). The billets were placed into the extrusion die and covered loosely with a 5 mm long copper plug to make sure that the extruded sample was completely ejected from the hot die. In order to minimize the overall time of heat treatment upon compaction and avoid crystallization, the die was heated at a rate of 100 K/min up to 773 K and beyond at a rate of 40 K/min. When the extrusion temperature of 850 K was reached, a load of 100 kN was applied to the billet. The extrusion ratio was about 6:1, determined from the reduction of the sample cross section, i.e. the diameter of the extruded billet was reduced from 12 mm to 5 mm (4 mm diameter of magnetic alloy with a thickness of copper cladding of 0.5 mm).

The phases present in the melt-spun $Fe_{67}Co_{9.5}Nd_3Dy_{0.5}B_{20}$ ribbon and in the extruded bulk samples were analyzed by X-ray diffraction (XRD) with Co-K_α radiation ($\lambda = 0.17889$ nm) using a Philips PW 3020 diffractometer. The thermal stability of the as-spun ribbon and the extruded samples was characterized by a differential scanning calorimeter (Perkin-Elmer DSC 7) under flowing high purity Ar using a heating rate of 40 K/min. The magnetic properties of the different samples were measured by a vibrating sample magnetometer with a maximum field of 2.0 T (Lakeshore-7300 VSM).

3. Results and discussion

Fig. 1 shows the XRD pattern for the melt-spun $Fe_{67}Co_{9.5}Nd_3Dy_{0.5}B_{20}$ ribbon. The diffraction pattern consists of a broad maximum and no appreciable diffraction peaks corresponding to crystalline phases are detected, indicating the amorphous structure of the as-spun ribbon.

Fig. 2 shows the DSC thermogram recorded upon constant-rate heating the $Fe_{67}Co_{9.5}Nd_3Dy_{0.5}B_{20}$ ribbon to 960 K at 40 K/min heating rate. The thermogram shows an endothermic event, which is characteristic of a glass transition with glass transition temperature (T_g) (determined as the onset temperature of the endothermic DSC event) and a distinct supercooled liquid region before the onset of crystallization at a temperature T_x, as well as two crystallization events with peak temperatures (T_{p1}, T_{p2}). The values of T_g, T_x, T_{p1}, T_{p2} and the extent of the supercooled liquid region ΔT_x ($= T_x - T_g$), as well as the

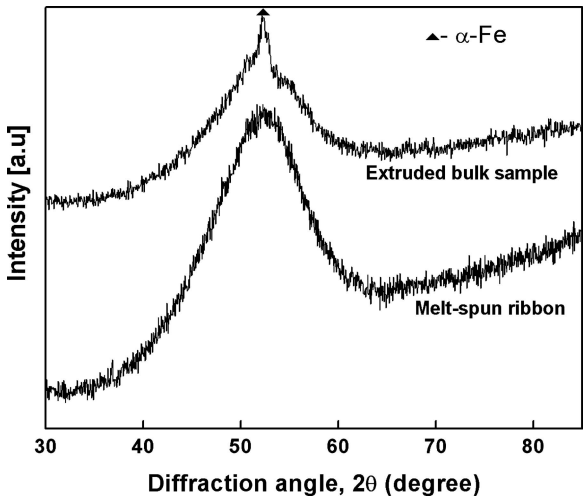

Figure 1 X-ray diffraction patterns for $Fe_{67}Co_{9.5}Nd_3Dy_{0.5}B_{20}$ in the form of melt-spun ribbon and an extruded bulk sample (extruded at 850 K).

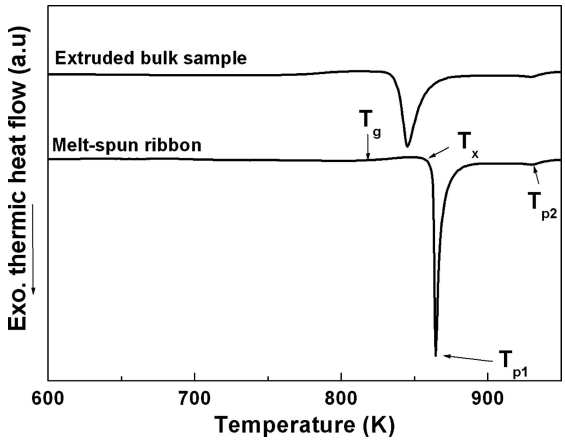

Figure 2 DSC scans (heating rate 40 K/ min) for $Fe_{67}Co_{9.5}Nd_3Dy_{0.5}B_{20}$ melt-spun ribbon and an extruded bulk sample (extruded at 850 K).

exothermic enthalpy release upon crystallization (ΔH_{x1}, ΔH_{x2}) are listed in Table I for the ribbon and the extruded samples.

The first pronounced crystallization event with peak temperature T_{p1} corresponds to the crystallization of soft magnetic α-(FeCo) and $(FeCo)_3B$ phases and the second crystallization step at higher temperature (T_{p2}) corresponds to the formation of hard magnetic $(NdDy)_2(FeCo)_{14}B$. The first strong crystallization event is due to the structure change from the amorphous phase to α-(FeCo) + $(FeCo)_3B$ + remaining amorphous phases, and the second much weaker exothermic peak results form the change from α-(FeCo) + $(FeCo)_3B$ + remaining amorphous to α-(FeCo) + $(FeCo)_3B$ + $(NdDy)_2(FeCo)_{14}B$ + remaining amorphous phases.

Optimum heat treatment can yield good hard magnetic properties due to the exchange coupling between hard and soft magnetic phases coexisting with a residual amorphous phase, presumably because of the maintenance of the finely mixed structure [23]. The as-quenched ribbons were annealed at 903 K (i.e. in the temperature range between the first and the second crystallization peak) and 973 K (i.e., above the second crystallization peak temperature) for 7 min, in each case. These annealing time and temperature parameters were used since it has been already reported by Zhang *et al.* [12] and Parida *et al.* [15] that these annealing conditions yield optimum hard magnetic properties for $Fe_{67}Co_{9.5}Nd_3Dy_{0.5}B_{20}$ ribbon.

The XRD patterns for the ribbon annealed at 903 K and 973 K for 7 min are shown in Fig. 3. The patterns show that bcc α-(FeCo) and tetragonal $(FeCo)_3B$ phases were developed in the sample, which was annealed at 903 K. When the sample was annealed at 973 K, the $(NdDy)_2(FeCo)_{14}B$ phase started to form. The intensity of the XRD peaks corresponding to the $(NdDy)_2(FeCo)_{14}B$ phase increases with increasing annealing temperature and time [24], indicating an increased volume fraction of this hard magnetic phase. The optimally annealed alloy contains a mixture of α-(FeCo) + $(FeCo)_3B$ + $(NdDy)_2(FeCo)_{14}B$ + remaining amorphous phase. The grain size of the crystalline products for the sample annealed at 973 K for 7 min was determined by analyzing the broadening of the X-ray diffraction peaks using the Scherrer equation [25], $D = 0.9\lambda/\beta \cos\theta$, where D is the crystallite size, λ is the wavelength of the incident radiation, and β is the full width at half maximum of the corresponding peak after correcting for the peak broadening which is caused by the diffractometer. The calculated grain size is 19 nm for α-(FeCo), 22 nm for $(FeCo)_3B$ and 16 nm for $(NdDy)_2(FeCo)_{14}B$.

The hysteresis loop for the as-spun $Fe_{67}Co_{9.5}Nd_3Dy_{0.5}B_{20}$ ribbon is shown in Fig. 4. It exhibits a J_s of 1.26 T and almost zero H_c. This finding is consistent with the result obtained from XRD indicating an amorphous structure. Fig. 4 also shows the hysteresis loop for the ribbon after annealing at 903 K for 7 min, which shows a similar behavior to that of the as-spun ribbon. This indicates the absence of any hard magnetic phase after annealing the sample just below T_{p2}. However, Fig. 4 shows the hysteresis loop for the ribbon after annealing at 973 K for 7 min, which reveals hard magnetic properties ($B_r = 1.01$ T, $H_c = 200$ kA/m and $J_s = 1.35$ T). The hard magnetic properties of this sample may be attributed to the exchange coupling interaction between the soft and hard magnetic phases in the sample, which

TABLE 1 Thermal stability data (heating rate 40 K/min) for $Fe_{67}Co_{9.5}Nd_3Dy_{0.5}B_{20}$ ribbon and extruded samples (extruded at 850 K)

Sample	T_g (K)	T_x (K)	T_{p1} (K)	ΔT_x	T_{p2} (K)	ΔH_{x1} (J/g)	ΔH_{x2} (J/g)
Melt-spun ribbon	819 (±1)	863 (±1)	865 (±1)	44	929 (±1)	−98 (±2)	−12 (±2)
Extruded Sample	774 (±1)	834 (±1)	845 (±1)	60	929 (±1)	−91 (±2)	−11 (±2)

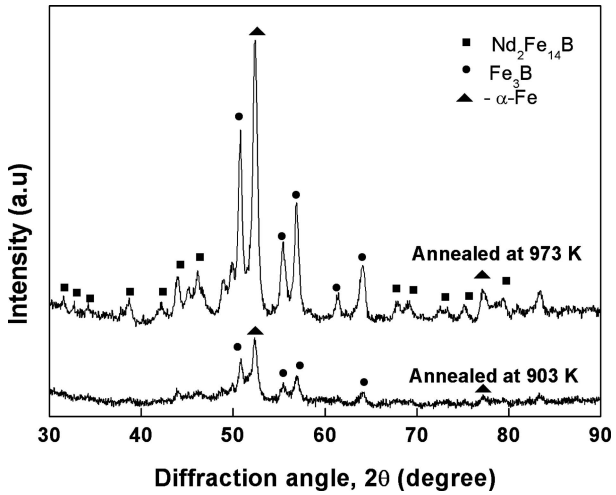

Figure 3 X-ray diffraction patterns for the $Fe_{67}Co_{9.5}Nd_3Dy_{0.5}B_{20}$ ribbon after isothermal annealing at 903 K and 973 K for 7 min.

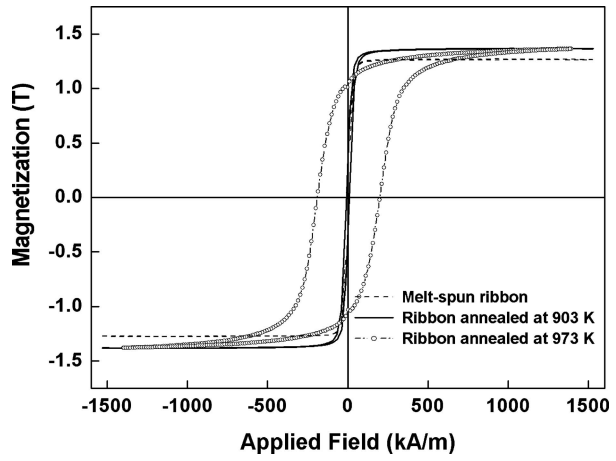

Figure 4 Hysteresis loops for the as-spun $Fe_{67}Co_{9.5}Nd_3Dy_{0.5}B_{20}$ ribbon and for annealed ribbons after isothermal annealing at 903 K and 973 K for 7 min.

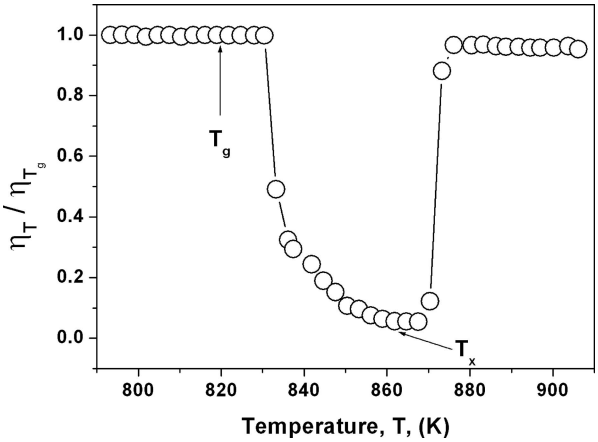

Figure 5 Plot of normalized viscosity (η_T /η_{Tg}) vs. temperature for amorphous $Fe_{67}Co_{9.5}Nd_3Dy_{0.5}B_{20}$ powder. The data were obtained by parallel plate rheometry at a constant heating rate of 40 K/min.

was confirmed by X-ray diffraction studies revealing the presence of soft magnetic α- (FeCo) and $(FeCo)_3B$ as well as hard magnetic $(NdDy)_2(FeCo)_{14}B$ in the annealed sample Fig. 3.

With the aim of understanding the viscous flow behavior of the supercooled liquid in order to prepare extruded samples, viscosity measurements were performed on the ball milled powder obtained from the crushed ribbons. Viscous flow in the supercooled liquid region is one of the useful characteristics of amorphous metallic alloys, that can be utilized to easily prepare bulk samples by extrusion or other hot working techniques [18]. In Fig. 5, the normalized viscosity (η_T /η_{Tg}), i.e., the ratio of the viscosity at temperature T to the viscosity at the temperature of the calorimetric glass transition T_g, as measured by parallel plate rheometry, is plotted as a function of temperature T using a heating rate of 40 K/min. The T_g and T_x values determined from the DSC scan recorded at the same heating rate are marked in the figure by arrows. The viscosity starts to decrease when passing from the amorphous solid into the supercooled liquid region, as has been previously shown for a variety of metallic glasses [26]. When the temperature is further increased and crystallization sets in, the viscosity increases again. Thus, the viscosity drop in the supercooled liquid region can be utilized for rather easy consolidation/extrusion of the material, as long as massive crystallization is avoided.

A typical X-ray diffractogram for a sample extruded at 850 K is shown in Fig. 1. There are additional very weak diffraction peaks superimposed on the broad diffraction maximum of the amorphous phase. This is due to the formation of nanocrystalline α-(FeCo) precipitates coexisting with the glass. The formation of these nanocrystals can be explained from the work-induced heat generation during extrusion. The work-induced heat generation causes a temperature rise in the billet during extrusion [27]. This can be estimated according to the empirical relation [28, 29]

$$\Delta T = 1.1 \times 10^4 V_e^{0.64} P_e/(\rho C_p), \qquad (1)$$

with V_e = ram speed, P_e = pressure during extrusion, ρ = bulk density of the sample and C_p = specific heat of the sample.

With a ram speed 0.2 mm/s, an extrusion pressure of 0.895 GPa, a sample density of 7.3 g/cm^3 and a specific heat of 15 J/mol/K, Equation (1) gives a temperature rise of about 32 K. Adding this temperature to the extrusion temperature of 850 K, the actual temperature that the sample experienced upon extrusion was about 882 K, which is higher than the temperature of the crystallization peak (865 K). This temperature rise essentially accelerates the time-dependent incubation of the transformation.

The DSC thermogram for the extruded sample is included in Fig. 2. It shows a shift of T_g and T_{p1} to lower temperatures compared to the as-quenched ribbon. The different values of T_g, T_x, T_{p1}, T_{p2}, ΔT_x, ΔH_{x1} and ΔH_{x2} for the extruded specimen are listed in Table I. The shift in T_g, T_{x1} and T_{p1} is most likely due to the change in composition of the amorphous phase induced by the nanocrys-

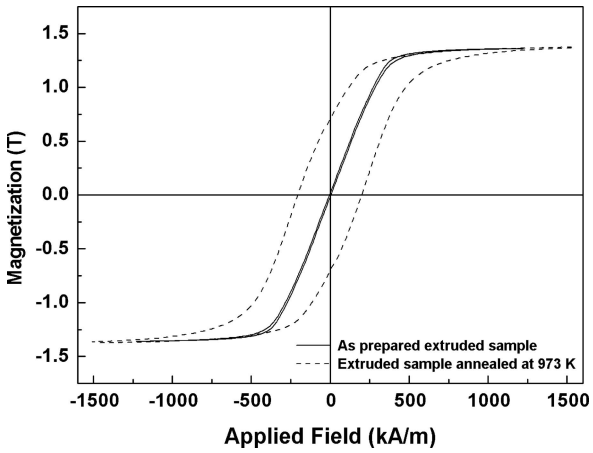

Figure 6 Hysteresis loop for an $Fe_{67}Co_{9.5}Nd_3Dy_{0.5}B_{20}$ as-extruded sample and for a sample after additional isothermal annealing at 973 K for 7 min.

tallization of α-(FeCo), which occurs during the extrusion process. Thus, the residual glassy phase becomes depleted in Fe, which shows a lower T_g and T_{p1}. The crystallization enthalpy decreases from 98 J/g for the as-quenched ribbon to 91 J/g for the extruded bulk sample. This also proves that nanocrystallization occurs during extrusion.

Fig. 6 shows the hysteresis loop for the as-extruded sample and that for the extruded sample following annealing at 973 K for 7 min. Obviously, the bulk sample also shows no hard magnetic properties. The coercivity of the extruded sample is 4.3 kA/m, which is higher than that for the as-spun ribbon. This can be explained from the X-ray diffraction results which suggest the existence of some nanosized α-(FeCo) crystallites in the amorphous phase. Apparently the partial crystallization induced upon extrusion does not lead to hard magnetic properties. A higher extrusion temperature may lead to complete crystallization without the presence of residual amorphous phase, which is undesirable for hard magnetic properties together with enhanced remanence. Thus, additional annealing treatment is necessary in order to partially crystallize the sample while still maintaining a residual amorphous phase. The extruded sample that was annealed at 973 K for 7 min exhibits hard magnetic properties with $H_c = 218$ kA/m, $J_s = 1.36$ T, $B_r = 1.18$ T and $(BH)_{max} = 91.3$ kJ/m^3 after demagnetization field correction with a demagnetization factor of 0.23 [30]. These values are in the same range as those for bulk samples prepared by uniaxial hot pressing [14–15].

The differences in the shape of the hysteresis loops for the extruded sample and the as-quenched ribbon can be explained by the difference of the demagnetizing factor for the ribbons and the extruded sample. At a particular applied field, the magnetization in the as-cast ribbon is higher than the magnetization in the extruded sample. The higher demagnetizing factor in the extruded bulk sample is responsible for this behavior. The demagnetizing field depends on two factors only. These are the magnetization in the material and the shape of the specimen. The demagnetizing field is proportional to the magnetization and is given by the expression [30]:

$$H_d = N_d M, \tag{2}$$

where N_d is the demagnetizing factor, which is calculated solely from the sample geometry. In the case of the ribbon, the value of the demagnetizing factor is very low (< 0.00617) compared to the extruded bulk sample (0.23) [30].

4. Conclusions

$Fe_{67}Co_{9.5}Nd_3Dy_{0.5}B_{20}$ bulk amorphous samples were prepared by extrusion of powder obtained form crushed ribbons. DSC analysis and X-ray diffraction studies showed that the devitrification of this alloy occurs in two stages. The first crystallization step corresponds to the precipitation of soft magnetic α-(FeCo) and $(FeCo)_3B$ from the amorphous matrix while the second crystallization step at higher temperature corresponds to the crystallization of hard magnetic $(NdDy)_2(FeCo)_{14}B$ from the residual amorphous phase. The as-quenched ribbon has almost zero coercivity and soft magnetic properties Annealing at 973 K for 7 min yields hard magnetic properties due to the exchange interaction between soft and hard magnetic phases. The extruded sample also exhibits similar hard magnetic properties when it is annealed at optimum temperature. H_c, J_s, B_r and $(BH)_{max}$ are 218 kA/m, 1.36 T, 1.18 T and 91.3 kJ/m^3 respectively after demagnetisation field correction with a demagnetisation factor of 0.23, for the extruded bulk sample that was subsequently annealed at 973 K for 7 min. The bulk extruded $Fe_{67}Co_{9.5}Nd_3Dy_{0.5}B_{20}$ alloy is promising for magnetic applications because of its high values of remanence and coercivity when it is annealed at optimum temperature.

Acknowledgements

The authors thank F. Schurack for stimulating discussions. K. Biswas is grateful for the financial support provided by the "DAAD-IIT Masters Sandwich Program" for his stay at the IFW Dresden.

References

1. J. J. CROAT, J. F. HERBST, R. W. LEE and F. E. PINKERTON, *J. Appl Phys.* **55** (1984) 2078.
2. M. SAGAWA, S. FUJIMURA, N. TOGAWA, H. YAMAMOTO and Y. MATSUURA, *ibid.* **55** (1984) 2083.
3. N. C. KOON, B. N. DAS, M. RUBINSTEIN and J. TYSON, *ibid.* **57** (1985) 4091.
4. G. C HADJIPANAYIS, R. C. HAZELTON and K. P. LAWLESS, *ibid.* **55** (1984) 2073.
5. L. SCHULTZ and J. WECKER, *Mater. Sci. Eng.* **99** (1988) 127.
6. R. COEHOORN, D. B. DE MOOIJ, J. P. W. B. DUCHATEAU and K. H. J. BUSCHOW, *J. Phys.* **49** (1988) 669.
7. E. F. KNELLER and R. HAWIG, *IEEE Trans. Magn.* **27** (1991) 3588.
8. A. MANAF, R. A. BUCKLEY and H. A. DAVIES, *J. Magn. Magn. Mater.* **128** (1993) 302.

9. H. KANEKIYO, M. UEHARA and S. HIROSAWA, *IEEE Trans. Magn.* **29** (1993) 2863.
10. R. K. MISHRA and V. PANCHANATHAN, *J. Appl. Phys.* **75** (1994) 6652.
11. L. WITHANAWASM, A. S. MURPHY, G. C. HADJIPANAYIS and R. F. KRAUSE, *ibid.* **76** (1994) 7065.
12. W. ZHANG and A. INOUE, *ibid.* **87** (2000) 6122.
13. Idem., *Appl. Phys. Lett.* **80** (2002) 1610.
14. S. ISHIHARA, W. ZHANG and A. INOUE, *Scripta Mater.* **47** (2002) 231.
15. S. PARIDA, S. RAM, J. ECKERT, S. ROTH, W. LÖSER and L. SCHULTZ, *Mater. Lett.* **58** (2004) 1844.
16. C. SURYANARAYANA, in "Materials Science & Technology (A comprehensive treatment)", edited by R. W. CAHN, P. HAASEN and E. J. KRAMER (VCH Publisher Inc., New York, 1991) p. 102.
17. K. BISWAS, S. RAM, L. SCHULTZ and J. ECKERT, *J. Alloys & Compd.* **397** (2005) 104.
18. J. ECKERT, *Mater. Sci. Eng. A* **226–228** (1997) 364.
19. M. J. STEFAN, *Akad. Wiss. Lit. (Mainz), Math. Naturwiss. Kl.* **69** (1874) 713.
20. G. J. DIENNES and H. F. KLEMM, *J. Appl. Phys.* **17** (1946) 458.
21. A. KÜBLER, J. ECKERT, A. GEBERT and L. SCHULTZ, *ibid.* **83** (1998) 3438.
22. J. ECKERT, A. KÜBLER and L. SCHULTZ, *ibid.* **85** (1999) 7112.
23. W. ZHANG, M. MATSUSHITA and A. INOUE, *ibid.*. **89** (2001) 492.
24. K. BISWAS, *M. Tech Dissertation*, Indian Institute of Technology, Kharagpur, April 2003.
25. M. P. KLUG and L. F. ALEXANDER, in "X-Ray Diffraction Procedures for Polycrystalline and Amorphous Materials" (John Wiley & Sons, New York, 1974) p. 634.
26. R. BUSCH, E. BAKKE and W. L. JOHNSON, *Act. Mater.* **46** (1998) 4725.
27. F. SCHURACK, J. ECKERT and L. SCHULTZ, *Phil. Mag.* **83** (2003) 807.
28. W. JOHNSON, *J. Inst. Metals.*, **85** (1956) 403.
29. Y. KAWAMURA, A. INOUE, K. SASAMORI and T. MASUMOTO, *Mater. Sci. Eng.* **A181–182** (1994) 1174.
30. D. JILES, in "Introduction to Magnetism and Magnetic Materials" (Chapman & Hall, London, 1996) p. 38.

Received 26 April 2005
and accepted 22 July 2005